JOURNAL OF
EMERGING INVESTIGATORS

Article

The novel function of *PMS2* mutation on ovarian cancer proliferation

Yoonseo Cho[1], Woo Rin Lee[2]

[1] Singapore American School, Singapore

[2] Department of Biological Science, University of Suwon, Wau-ri, Bongdam-eup, Hwaseong, Gyeonggi-do, Republic of Korea

SUMMARY

The *PMS2* gene encodes a protein that plays an essential role in repairing DNA. Recent studies have shown that the S815L *PMS2* mutation, rarely found in ovarian cancer (3%), causes a reduction in the PMS2 protein's mismatch repair activity in vitro. However, no studies have focused on how this mutation affects cancer progression. Although occurrences of patients with cancers associated with the *PMS2* mutation are rare, the lack of studies published on this mutation still negatively impacts their treatment. Our study aimed to discover the novel effect of this mutation in ovarian cancer cells. We hypothesized that overexpressing the wild-type *PMS2* gene would have tumor-suppressive effects while overexpressing S815L *PMS2* mutant would negatively affect ovarian cancer cell proliferation. We tested three transfection conditions: pcDNA3 as a negative control variant, wild-type pcDNA3-PMS2, and pcDNA3-PMS2 mutated vectors. Using RT-PCR analysis, we optimized the transfection conditions for overexpression of both the wild-type *PMS2* and mutant genes in OVCAR-3 cells. We acquired microscopic images to observe cell morphology and colonization. Also, we performed a Prestoblue assay to quantify the number of live cells in each condition. Results showed that the pcDNA3-PMS2 mutated vector has a higher cell proliferation than the wild-type vectors. As hypothesized, overexpressing the wild-type *PMS2* gene had tumor-suppressive effects. This observation shows that the pcDNA3-PMS2 mutation has a tumor-progressive impact on the OVCAR-3 cells. Overall, we conclude that the *PMS2* mutation has tumor-progressive effects in ovarian cancer cells while the unmutated version of the gene does not.

INTRODUCTION

Ovarian cancer is notorious for being diagnosed in its advanced stages due to its vague but detrimental symptoms that are difficult to detect (1). This leads to many patients suffering through painful symptoms while cancer's malignant behavior spreads to surrounding organs (2). Survival rates for this gynecological cancer are also extremely low, as only approximately half of patients live for more than five years after diagnosis (3). One principal cause for ovarian cancer comes from a germline mutation, also known as a hereditary genetic disorder, that passes through to the DNA to offspring (4).

The *PMS2* S815L mutation causes near or complete loss of the PMS2 protein ability to carry out mismatch repair tasks for healthy cell growth (5). Due to increased degradation of the mutant protein, S815L PMS2 protein remained at low levels in the cell (5). As a result, individuals who test positive for this mutation have Lynch syndrome (LS), also known as hereditary non-polyposis colorectal cancer (HNPCC) (6). Statistically, individuals with the S815L *PMS2* gene mutation face a 10-20% colorectal cancer risk, almost four times the risk of an individual who does not carry this mutation (4%) (6). Similarly, a woman with the *PMS2* gene mutation (S815L) has a drastically higher risk of endometrial cancer (15–25%) than an individual who does not carry this mutation (3%) (7).

S815L *PMS2* is a single nucleotide variant that causes missense mutation. The serine at amino acid position 815 is replaced by leucine in the S815L PMS2 protein. A high yield of *PMS2* germline heterozygous mutations is associated with the isolated loss of PMS2 expression (8). Moreover, the most evident study published regarding LS-related cancers did not report a single S815L *PMS2* heterozygous mutation case (5). Due to the lack of comprehensive information about S815L *PMS2* mutation occurrences, it is crucial to study the functional effects of the S815L *PMS2* mutation in ovarian cancer progression. Therefore, the purpose of our research was to expand our knowledge of this rare mutation to allow for more research to be conducted on the correlation between the *PMS2* mutation and ovarian cancer.

Previous experimental studies have shown that this mutation causes a significant reduction in S815L *PMS2* mismatch repair activity *in vitro* (8). However, there are no known studies on the function of wild-type *PMS2* and *PMS2* (S815L) in the context of ovarian cancer progression. Therefore, we overexpressed wild-type and S815L *PMS2* mutation in ovarian cancer cells (OVCAR-3) to examine its effect on cell proliferation to test our hypothesis that the PMS2 mutated protein would have tumor-progressive effects while the PMS2 wild-type protein would have tumor-suppressive effects.

RESULTS

In the S815L *PMS2* gene, there are 15 exons in total, and the location of the *PMS2* c.2444 C>T mutation is located at the end of exon 14 (**Figure 1**). The length of the *PMS2* coding sequence is 2589 base pairs (bp).

We aimed to overexpress *PMS2* wild-type and S815L *PMS2* mutants in OVCAR-3 cells to analyze the function of these genes. We transfected OVCAR-3 cells with pcDNA3 vector containing a cytomegalovirus (CMV) promoter controlling expression of the S815L *PMS2* or S815L *PMS2* c.2444 C>T mutant gene as a constitutive promoter. We expected that the

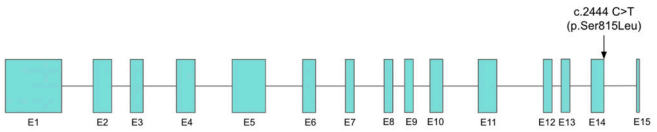

Figure 1. Position of c.2444 C>T (p.Ser815Leu) mutation on PMS2 gene. Box represents the exon with the number, and the line represents the introns. The arrow indicates the position of the c.2444 C>T (p.Ser815Leu) mutation.

transfection of pcDNA3-PMS2 wild-type and pcDNA3-PMS2 mutant vectors would result in overexpression of the S815L *PMS2* gene. Therefore, to compare the expression level of the S815L *PMS2* gene, we extracted RNA from transfected OVCAR-3 cells, followed by cDNA synthesis and amplification of *PMS2* and *GAPDH* by PCR. Finally, we performed agarose gel electrophoresis to visualize the amplified band of *PMS2* and *GAPDH*.

As hypothesized, compared to the pcDNA3 band, both the pcDNA3-PMS2 wild-type and pcDNA3-PMS2 mutant vector bands showed a stronger band on *PMS2* (**Figure 2**). Furthermore, the pcDNA3-PMS2 mutant vector displays a slightly stronger band on *PMS2* than the pcDNA3-PMS2 wild-type vector (**Figure 2**). This result indicates that both wild-type and the S815L *PMS2* mutant were successfully overexpressed in OVCAR-3 cells.

Next, we acquired microscopic images of the pcDNA3, wild-type pcDNA-PMS2, and pcDNA3-PMS2 in order to observe the cell quantities and viability in each transfection condition. Comparing the pcDNA3 and pcDNA3-PMS2 wild-type vector-transfected conditions, there was a visibly lower concentration and number of colonies of cells in the *PMS2* wild-type transfected cells (**Figure 3**). In addition, between the pcDNA3 and pcDNA3-PMS2 mutant vectors, there were more cells and colonies, groups of multiple cells, observed in the pcDNA3-PMS2 mutant transfected cells (**Figure 3**). Last, there was a noticeable and dramatic change in cell concentration and aggregation between the pcDNA3-PMS2 wild-type and mutant vectors (**Figure 3**). Specifically, the pcDNA3-PMS2 mutant vector had a higher concentration and aggregation of ovarian cancer cells than the wild-type vector. This result indicates that the *PMS2* wild-type gene and S815L mutant may have opposite effects on the proliferation of cancer cells.

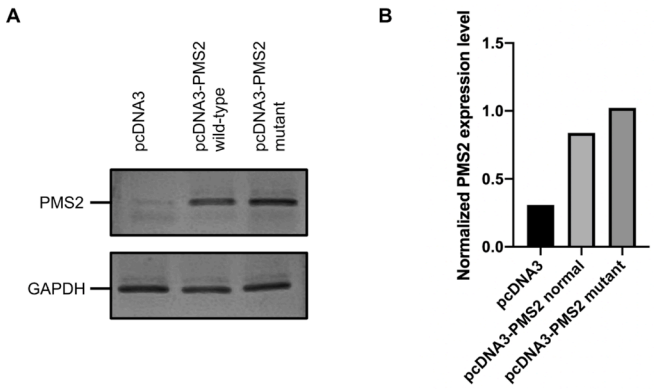

Figure 2. Both PMS2 wild-type and mutant cloned pcDNA3 vectors overexpressed the PMS2 gene in OVCAR-3 cells. (A) Agarose gel image showing amplified PMS2 and GAPDH cDNA. OVCAR-3 cells were transfected with either pcDNA3, wild-type pcDNA3-PMS2, or pcDNA3-PMS2 mutant and incubated for 48 hours. (B) Bar graph showing normalized PMS2 expression level. GAPDH expression level was used to normalize PMS2 expression level.

To observe the number of live cells after each vector transfection, we stained the cells using Acridine Orange (AO) and Propidium Iodide (PI) stains. The AO fluorescence (green) is found in live cells only while the PI fluorescence (red) is found in dead cells only; hence, the green cells represent live cells and the red cells represent dead cells in each vector. Using a LUNA-FL™ Automated Fluorescence Cell Counter, the number of live (green) cells in each vector can be quantified. Through this analysis, the pcDNA3-PMS2 mutant showed the highest number of live cells in the image while the pcDNA3-PMS2 wild-type showed the lowest number of live cells in the image (**Figure 4**). To support these observations, we also quantified the number of live, dead, and total cell concentrations in each condition (**Table 1**). Specifically, the live cell concentration in the pcDNA3 vector condition was 2.51×10^6 cells/mL, 1.72×10^6 cells/mL in the pcDNA3-PMS2 wild-type vector condition, and 3.07×10^6 cells/mL in the pcDNA3-PMS2 mutant vector condition. Following our prior observations in the cell images, the live cell concentration was the highest in the pcDNA3-PMS2 mutant condition while the live cell concentration is the least in the pcDNA3-PMS2 wild-type condition (**Table 1**).

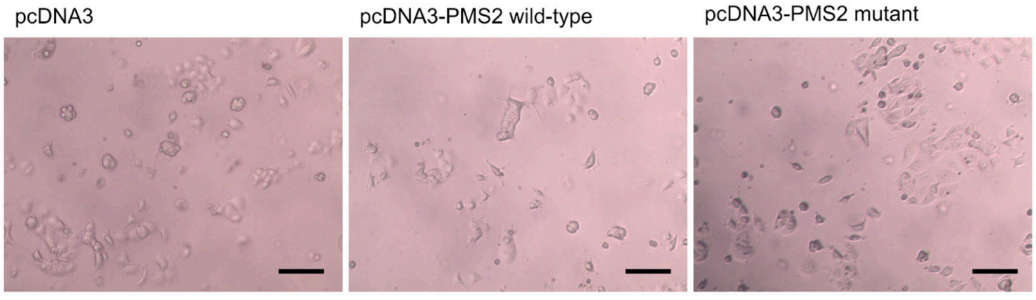

Figure 3. Overexpressed PMS2 wild-type decreased the number of cancer cells, but overexpressed PMS2 mutants increased the number of cancer cells. Images showing visible effects of the PMS2 gene on the proliferation of ovarian cancer cells. After cells were transfected by either pcDNA3 (left), wild-type pcDNA3-PMS2 (middle), or pcDNA3-PMS2 mutant (right), brightfield microscopic images were taken to observe the live cells attached to the culture plate. Scale bar = 50 μm.

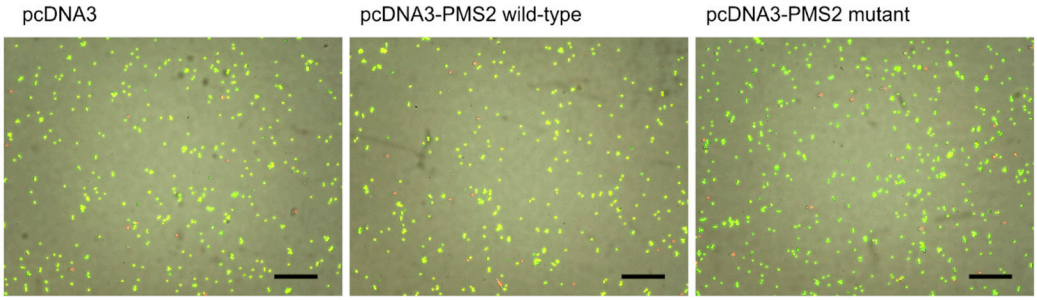

Figure 4. Overexpression of wild-type and mutated PMS2 has a differential effect on cancer cell viability. 72 hours after the cells were transfected with either pcDNA3, wild-type pcDNA3-PMS2, or pcDNA3-PMS2 mutant, the live cells (green) and dead cells (red) were analyzed after acridine orange/propidium iodide staining. Scale bar = 50 μm.

To identify the functional effect of the *PMS2* wild-type and S815L mutant on cancer progression, we performed a cancer cell proliferation assay, which fundamentally evaluates the advancement of tumor size. We measured the absorbance at 570 and 600 nm for each of the cell cultures of transfected cells. We used a Prestoblue reagent to quantify the cancer cell proliferation and incubating this reagent with the cancer cells increased the light absorbance on 570 nm wavelength. Therefore, the 570 nm absorbance is positively correlated with cancer cell proliferation. The results showed significant differences between all three vectors. pcDNA3-PMS2 wild-type vector (2.07 AU) decreased cell proliferation compared to the control variable, pcDNA3 (2.32 AU). (p = 0.0009, One-way ANOVA, **Figure 5**). In contrast, the pcDNA3-PMS2 mutant vector (3.61 AU) showed significantly increased cell proliferation than pcDNA3 control vector (p = 0.00008, One-way ANOVA, **Figure 5**). These observations lead to a conclusion that the *PMS2* wild-type gene may function as a tumor suppressor while the S815L *PMS2* mutant causes the loss of function mutation that leads to increased cancer cell growth.

DISCUSSION

In summary, the data derived from each experiment pointed towards a unified conclusion that the S815L *PMS2* mutation causes tumor progressive effects. First, we verified the overexpression of the *PMS2* wild-type and S815L *PMS2* mutant using RT-PCR. This test ensured that both vectors had observable effects on OVCAR-3 cells. Next, through our cell images, it was visible that there were more live aggregated cells in the overexpressed S815L *PMS2* mutant OVCAR-3 cells than in the overexpressed *PMS2* wild-type OVCAR-3 cells. Also, we observed that the overexpressed S815L *PMS2* mutated cells had increased cell proliferation than both the control vector and the overexpressed *PMS2* wild-type cells. Last, our final experimental results aligned with our original hypothesis as the S815L *PMS2* mutation showed tumor progressive effects, while the *PMS2* wild-type gene did not.

Several limitations restricted the results and impact of this study. Firstly, we used only one ovarian cell line to investigate the effect of the *PMS2* gene and the S815L *PMS2* mutant on ovarian cell proliferation in this study. To further confirm our findings, we can test more cell lines. Next, cell proliferation was our main investigation in this study. However, in the future, more cancer functions, including cell migration, cell invasion, cell death, and angiogenesis should be tested to expand knowledge on the S815L *PMS2* gene mutation. Moreover, we investigated the effects of S815L *PMS2* gene mutation only using mRNA. Thus, further analysis of protein levels is necessary to ensure more accurate results. Additionally,

	Live cell concentration (cells/ml)	Dead cell concentration (cells/ml)	Total cell concentration (cells/ml)	Viability % (live/total)
pcDNA3	2.51 x 10^6	3.82 x 10^4	2.55 x 10^6	98.5%
wild-type pcDNA3-PMS2	1.72 x 10^6	2.52 x 10^5	1.97 x 10^6	87.2%
pcDNA3-PMS2 mutant	3.07 x 10^6	4.36 x 10^4	3.12 x 10^6	98.6%

Table 1. Quantification result of live cell, dead cell, and total cell concentrations. The average concentration of live, dead, and total cells of three biological replicates are presented (n=3). LUNA-FL fluorescent cell counter device was used to count the live and dead cells.

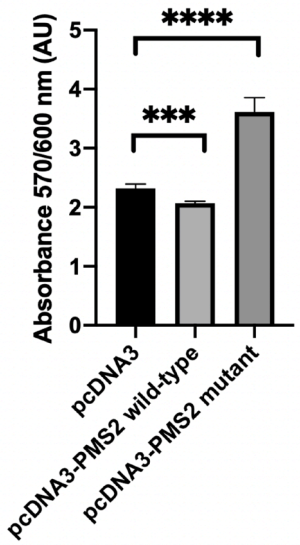

Figure 5. The overexpressed wild-type PMS2 vector decreased the cancer cell proliferation, but the overexpressed PMS2 mutant vector increased the cancer cell proliferation. Bar graph showing mean ± standard deviation (SD) of absorbance 570/600 nm (Arbitarty Unit, AU) representing the viable cells (n=3). After cells were transfected by either pcDNA3, wild-type pcDNA3-PMS2, or pcDNA3-PMS2 mutant, prestoblue assay reagent was added to each sample and was incubated for 1 hour. One-way ANOVA with Tukey's post hoc test, ***p < 0.001, ****p < 0.0001.

since we did not sequence PMS2 in our OVCAR-3 cells, nor were there available databases, the endogenous *PMS2* gene information is unknown. To further investigate the function of both the endogenous *PMS2* and S815L mutant *PMS2*, sequencing information would be vital for data interpretation in future studies. Also, our overexpression condition showed that the S815L *PMS2* expression was slightly higher than the wild-type *PMS2* expression. Since the protein level was not normalized, our result can be varied by the protein concentrations of both wildtype and S815L mutant PMS2. Also, even though we added the same concentration of the cells for each transfection condition, we did not actually count the initial cell number before the transfection. Moreover, we were unable to carry out biological replicates which would have increased the transfection efficiency. Last, we only performed *in vitro* experiments, meaning that our results represent limited conditions for the actual tumors. Therefore, it is necessary to perform mouse experiments (*in vivo*) to verify our results and learn more about the effects of these mutations.

Prior to this study, we found no information on the effects of both the S815L *PMS2* gene and *PMS2* c.2444 C>T mutant on ovarian cancer progression. Therefore, our study investigated the functional role of the *PMS2* gene and the *PMS2* mutation on ovarian cancer cell proliferation for the first time. Additionally, our study results directly align with research previously conducted on the functional role of the *PMS2* gene (9). This study showed that the *PMS2* wild-type gene caused decreased cell proliferation, migration, and *in vivo* growth compared to the control vector. Similarly, our study also showed that the *PMS2* gene had a tumor-suppressive role in ovarian cells, significantly consistent between both experiments. We understand that a wild-type tumor suppressor gene would carry the functions of regulating the cell cycle through apoptosis such as PMS2, and loss of function mutation in these genes causes uncontrolled cell growth or cancer. However, the gain of function mutation on the *PMS2* gene may increase the cell viability in our study. Similarly, overexpressing *PMS2* in ovarian cancer may increase the viability of our cell model. Also, it is possible that the overexpressed *PMS2* S815L will have an inhibitory effect on endogenous wildtype *PMS2*, showing a dominant-negative effect. For example, mutant p53 can have a dominant-negative effect over wild-type p53 by preventing wild-type p53 from binding to the promoter region of its downstream target genes (10). In conclusion, our study further expanded knowledge on the S815L *PMS2* gene mutation and its effect on ovarian cell lines. Not only does our finding allow for more in-depth studies conducted on the mutation *in vitro*, but the results also provide a biological understanding of the nature of *PMS2* mutations. These observations are necessary for developing treatments and prevention for those prone to ovarian cancer due to the *PMS2* mutation. Thus, utilizing this novel information can provide more efficient treatment for ovarian cancer patients in the future.

MATERIALS AND METHODS

Cell Culture and Maintenance

OVCAR-3, a human ovarian cancer cell line, was purchased from Korea Cell Line Bank (KCLB). OVCAR-3 cells were maintained in RPMI1640 medium (Gibco) supplemented with 10% fetal bovine serum (Thermofisher) and 1% penicillin and streptomycin (Thermofisher) and placed in a CO2 incubator (Effendorf) at 37 °C. Every three days, old media was removed by aspiration, and trypsin-EDTA solution was used to detach the cells from the culture plate. Then, 20% of the cells were seeded with fresh media into a new cell culture plate.

Plasmid DNA Transfection

To create vectors for transfections, separate plasmid DNA and Lipofectamine solutions were prepared by adding 3uL of plasmid DNA and 7uL Lipofectamine 2000 Reagent to 100 uL DMEM, respectively. Each of the DNA solutions was then added to the corresponding Lipofectamine-containing solutions. The tubes were then incubated for five minutes to allow the solutions to form a complex. After incubation, the DNA and Lipofectamine solutions were carefully combined into three labeled tubes: Empty Vector, Wild-type Vector, and Mutated Vector. Tubes were then incubated for another five minutes to form a complex. After that, mixed solutions were added to their corresponding labeled cell plates dropwise. After incubating the cells with the mixed solution for 3 hours, fresh media was added to the cells.

Cell Imaging with a Bright-field Microscope

OVCAR-3 cells were transfected with either pcDNA3, pcDNA3-PMS2 wild-type, or pcDNA3-PMS2 mutant vectors (provided by Prof. Woo Rin Lee from the University of Suwon) and were incubated for 48 hours. Then, the phase contrast image of transfected OVCAR-3 cells was photographed using an inverted bright-field microscope (Nikon). The morphological characteristics were analyzed for each transfected condition using a 10x objective.

Total RNA Extraction from Cells

After OVCAR-3 cells were transfected with either pcDNA3, pcDNA3-PMS2 wild-type, or pcDNA3-PMS2 mutant and incubated for 48 hours, RNA was extracted from the cells using AccuPrep® Universal RNA Extraction Kit (Bioneer, K-3140) with the following protocol. After the cells were harvested, 400 µL of RB Buffer was added to completely lysis the cells. Then, 300 µL of ethanol (80%) was added to precipitate the RNA. The samples were transferred to the RNA binding column in a 2 mL collection tube and centrifuged at 13,000 g for 20 sec. The flow-through was discarded. After 700 µL of RWA1 Buffer was added, the tubes were centrifuged at 13,000 g for 20 sec. After the flow-through solution was discarded, 500 µL of RWA2 Buffer was added and centrifuged at 12,000 g for 20 sec. RWA2 was used again to repeat the washing step. The samples were centrifuged once more at 13,000 g for 1 min to completely remove ethanol. Finally, the RNA binding column was transferred to a new 1.5 mL tube for elution and 50 µL of ER buffer was added. After 1 min incubation, the samples were centrifuged 10,000 g for 1 min.

cDNA Synthesis

cDNA was synthesized from the extracted RNA using TOPscript™ Reverse Transcriptase (Enzynomics, RT002S) with the following protocol. The 20 µL cDNA reaction mix was prepared for each sample. For each reaction, 2 µL of 10 x TOPscript RT buffer was added, 1 µL of TOPscript Reverse Transcriptase (200 units/µL) was added, 2 µL of dNTP mixture (2 mM each), 5 µg of RNA template was added, 1 µL of Oligo

(dT) (100μM) and 0.5 μL of RNase Inhibitor (40 units/μL) were added, and sterile water up to 20 μL was added. The following condition was used for the thermocycler (Bioneer, T100): 25 °C for 10 min, 45 °C for 60 min, 95 °C for 5 min, 4 °C for storage.

Polymerase Chain Reaction (PCR)

PMS2 wild-type, PMS2 mutant, GAPDH genes were amplified with AccuPower® PCR PreMix kit (Bioneer, K-2012). For each sample, 20 μL reaction volume was prepared with the following conditions: 1 μL of template DNA, 1 μL of forward primer (10 pmol/μL), 1 μL of reverse primer (10 pmol/μL), and 17 μL of deionized water. The following PCR temperature and time was used: 1) 95 °C for 5 min, 2) 95 °C for 20 sec, 3) 55 °C for 20 sec, 4) 72 °C for 30 sec, 5) repeat step 2 to 4 for 34 cycles. The following primer pair sequence was used to amplify *PMS2* gene: f5′ -TTTGCCGACCTAACTCAGGTT- 3′ and 5′ -CGATGCGTGGCAGGTAGAA- 3′. For amplifying the *GAPDH* gene the following primer sequence was used: 5′ -ACAACTTTGGTATCGTGGAAGG- 3′ and 5′ -GCCATCACGCCACAGTTTC- 3′.

Agarose Electrophoresis

100 mL of Tris-Borate-EDTA buffer was mixed with 1.3g of agarose powder (Intron) to make a 1.3% agarose solution. Then the mixture was microwaved to allow the agarose powder to be fully dissolved into the solution. Then 5 μL of RedSafe dye (Intron) was added and mixed well. The solution was added to the gel caster and was left to solidify into a clear gel block for 30 mins. Each of the amplified DNA samples were carefully inserted into each well. A 100V current was applied to the gel tank for 20 min to separate the amplified DNA product by its size. The gel was then placed on a blue light illuminator to visualize the DNA band, and the image of the gel was taken.

Cell Viability Assay (Prestoblue Assay)

After removing the old media, Trypsin buffer was immediately added to the cells. Cells were then incubated for 10 minutes to be detached from the cell plate. 1.5 mL tubes were prepared, and 400 μL of RPMI 1640 media was added to each tube. 200 μL of previously incubated cells were then added to each tube. 90 μL of these cells were equally distributed to four different wells of a 96 well plate. This step was repeated another two times representing Empty Vector, wild-type PMS2 Vector, and the PMS2 Mutated Vector. 10 μL of prestoblue reagent (Invitrogen) was then added to each well, and the cells were incubated for 30 minutes. After incubation, 570 nm of absorbance was measured using the Microspectrometer (Biotek). Then, 570 nm absorbance was normalized by 600 nm to quantify cell proliferation.

Fluorescence-based cell counting assay

After 72 hours of plasmid transfection, the cells were harvested into the 1.5 mL tube. To stain the cells, 18 μL of the cells were moved into a new 1.5 mL tube with 2 μL of acridine orange/propidium iodide staining solution which was then incubated for 5 minutes. The photon slides were used as disposable slides for cell counting for the LUNA-FL (Logos Bio). These slides were developed for the highly sensitive detection of fluorescent signals. 10 μL of a sample was applied to each chamber. Automatic cell counting with fluorescent images was analyzed by the LUNA-FL. The viability of the cells was automatically analyzed using the following equation: green fluorescent cells (live cells) / [green fluorescent cells (live cells) + red fluorescent cells (dead cells)].

Statistical Analysis

One-way ANOVA with Tukey's post hoc test was used to calculate the *p*-value for the statistical analysis. The Prism 8 software was used to graph and calculate the *p*-value. *P*-value less than 0.05 was considered statistically significant.

ACKNOWLEDGEMENTS

We are very grateful to our family and friends who have supported and encouraged us throughout this research. Additionally, we would like to thank the University of Suwon for allowing us to conduct the experiments in their laboratories.

Received: March 26, 2022
Accepted: July 13, 2022
Published: December 18, 2022

REFERENCES

1. Roett, Michelle A., and Patricia Evans. "Ovarian Cancer: An Overview." *American Family Physician*, vol. 80, no. 6, Sept. 2009, pp. 609–616.
2. Dilley, James, *et al*. "Ovarian cancer symptoms, routes to diagnosis and survival - Population cohort study in the 'no screen' arm of the UK Collaborative Trial of Ovarian Cancer Screening (UKCTOCS)." *Gynecologic Oncology*, vol. 158, no. 2, Aug. 2020, pp. 316–322, doi:10.1016/j.ygyno.2020.05.002.
3. Baldwin, Lauren A., *et al*. "Ten-year relative survival for epithelial ovarian cancer." *Obstetrics and Gynecology*, vol. 120, no. 3, Sept. 2012, pp. 612–618, doi:10.1097/AOG.0b013e318264f794.
4. Testa, Ugo, *et al*. "Ovarian Cancers: Genetic Abnormalities, Tumor Heterogeneity and Progression, Clonal Evolution and Cancer Stem Cells." *Medicines*, vol. 5, no. 1, Feb. 2018, doi:10.3390/medicines5010016.
5. González-Acosta, Maribel, *et al*. "Elucidating the Clinical Significance of Two PMS2 Missense Variants Coexisting in a Family Fulfilling Hereditary Cancer Criteria." *Familial Cancer*, vol. 16, no. 4, Oct. 2017, pp. 501–507, doi:10.1007/s10689-017-9981-1.
6. Ten Broeke, Sanne W., *et al.* "Cancer Risks for PMS2-Associated Lynch Syndrome." *Journal of Clinical Oncology*, vol. 36, no. 29, Oct. 2018, pp. 2961–2968, doi:10.1200/JCO.2018.78.4777.
7. Win, Aung Ko, *et al*. "Risks of Colorectal and Other Cancers after Endometrial Cancer for Women with Lynch Syndrome." *Journal of the National Cancer Institute*, vol. 105, no. 4, Feb. 2013, pp. 274–279, doi:10.1093/jnci/djs525.
8. van der Klift, Heleen M., *et al.* "Comprehensive Mutation Analysis of PMS2 in a Large Cohort of Probands Suspected of Lynch Syndrome or Constitutional Mismatch Repair Deficiency Syndrome." *Human Mutation*, vol. 37, no. 11, Nov. 2016, pp. 1162–1179, doi:10.1002/humu.23052.

9. Fukuhara, Shinichiro, *et al*. "Functional Role of DNA Mismatch Repair Gene PMS2 in Prostate Cancer Cells." *Oncotarge*t, vol. 6, no. 18, June 2015, pp. 16341–16351, doi:10.18632/oncotarget.3854.
10. Willis, Amy, *et al*. "Mutant P53 Exerts a Dominant Negative Effect by Preventing Wild-Type p53 from Binding to the Promoter of Its Target Genes." *Oncogene,* vol. 25, no. 23, 2004, pp. 2330-2338. doi:10.1038/sj.onc.1207396

Copyright: © 2022 Cho & Lee. All JEI articles are distributed under the attribution non-commercial, no derivative license (http://creativecommons.org/licenses/by-nc-nd/3.0/). This means that anyone is free to share, copy and distribute an unaltered article for non-commercial purposes provided the original author and source is credited.